Asian Journal of Chemistry; Vol. 33, No. 11 (2021), 2789-2795

ASIAN JOURNAL OF CHEMISTRY

https://doi.org/10.14233/ajchem.2021.23419

Preparation, Characterization and Applications of Chitosan-Nanosilica-Graphene Oxide Nanocomposite

A. Sahila Grace*[1] and G.S. Prabha Littis Malar[1]

Department of Chemistry & Research Centre, Scott Christian College (Autonomous) (Affiliated to Manonmaniam Sundaranar University, Tirunelveli), Nagercoil-629003, India

*Corresponding author: E-mail: sahilamuhu@gmail.com

Received: 17 July 2021; *Accepted*: 30 August 2021; *Published online*: 20 October 2021; AJC-20564

In present study, a simple low cost method was used to prepare chitosan-nanosilica-graphene oxide (CS-NSi-GO) nanocomposite. Nanosilica and graphene oxide were synthesized from coconut husk ash and chitosan was synthesized from shrimp shell. Nanosilica was synthesized from coconut husk ash with alkaline extraction using sodium hydroxide followed by precipitation method using sulphuric acid. Graphene oxide was synthesized from the oxidative treatment of the raw material of coconut husk ash. After the synthesis of silica, the carbonized graphite was collected and treated by modified Hummer's method. The CS-NSi-GO nanocomposite was prepared by condense polymerization method. Various analytical methods such as Fourier transform infrared (FTIR) spectroscopy, Fourier transform Raman (FT-Raman) spectroscopy, scanning electron microscopy (SEM), energy dispersive X-ray analysis (EDAX) and transmission electron microscopy (TEM) were used to characterize the CS-NSi-GO nanocomposite. Eventually antibacterial, antifungal, antioxidant and cytotoxicity of the prepared nanocomposite were also evaluated.

Keywords: Nanosilica, Chitosan, Graphene Oxide, Antioxidant, Cytotoxicity.

INTRODUCTION

Chitosan is one of the most important biological polymeric macromolecules broadly used in drug delivery systems and various field of applications due to their non-toxic, anti-bacterial, biocompatible and biodegradable hydrophilic polymer [1,2]. Chitosan and its derivatives possess attractive specific biological activities, which has a linear polysaccharide rich in amine (-NH_2) groups and good chemical reactivity as it has a number of hydroxyls (-OH) groups [3,4]. Silica nanoparticles are in use for various applications for the replacement of polymer based materials due to their higher biocompatibility [5]. Silica nanoparticles functionalized anticancer drugs are one of the new fields of interest and the silica nanoparticles covered with a polymer and chitosan was studied broadly [6]. Because of the negative surface potential of silica particles, it can be easily coated with a positive charged anticancer drug and used for drug delivery applications [7]. Silica materials have been used as potential applications for drug delivery systems due to their biocompatibility, large surface area, high pore volume, notable loading capacity and modifiable surface properties [8,9]. Silica may be either crystalline or amorphous in nature depending on the burning temperature. Several methods for the synthesis of SiO_2 nanoparticles have been reported including sol-gel, hydrothermal procedure and agricultural wastes [10].

Nowadays, researchers are interested towards graphene oxide, a novel 2D nanomaterial prepared from natural graphite, have been brought up in biomedical applications and highly potential nanoscale reinforcements for the next generation of nanocomposite materials [11]. It is the suitable materials with different functional groups and its interaction ability is the material due to its special properties, such as its large surface area, chemical stability and remarkable mechanical durability [12]. Graphene oxide has chemically reactive oxygen functionality on the basal layers (hydroxyl and epoxy groups) and their edges (carboxylic acid), which increases reactions with other different materials [13].

Chitosan combining with nanosilica (NSi) and graphene oxide to form hybrid composite material. Combining graphene oxide and nanosilica would generate a carrier to obtain syner-

gistic properties of both materials which can cause to load aromatic drug, by using π-π stacking interaction between drug and graphene oxide [14,15]. Silica contains various silanol groups (Si-OH) on its outer shell, which act as suitable nucleation and anchor points for the natural functionalization of silica [16]. The surface of graphene oxide was covered by silica to improve the hydrophilicity of composite [17]. Another material that has been studied in this study was chitosan, with functional groups of -OH and -NH_2 [18].

In this study, chitosan (CS), nanosilica (NSi) and graphene oxide (GO) combined a nanocomposite (CS-NSi-GO) nanocomposite material was prepared by using an environmental recycled nanosilica and graphene oxide synthesis from coconut husk and biodegradable chitosan. Various analytical methods (*i.e*. FT-IR, FT-Raman, SEM-EDAX and TEM) were used to characterize the CS-NSi-GO nanocomposite. Eventually, antibacterial, antifungal, antioxidant and cytotoxicity of the prepared nanocomposite were also evaluated.

EXPERIMENTAL

The chemicals *viz*. sodium hydroxide, sulfuric acid (98%), sodium nitrate, potassium permanganate, hydrogen peroxide (30%), hydrochloric acid (5%), ammonia solution, chitosan, and acetic acid (CH_3COOH) were purchased from Merck, USA.

Synthesis of nanosilica (NSi) particles: Coconut husk was collected, cleaned, dried and treated by thermal combustion under controlled condition at 600 ºC for 5 h. The coconut husk ash was treated with alkali extraction followed by acid treat-ment. The precipitate was washed several times with boiled distilled water to remove sulphate impurities and dried in a hot air oven. The powdered silica was refluxing with 6 N HCl for 3 h using sand bath. Then, it was dissolved in 2 N NaOH by continuous stirring for 24 h on a magnetic stirrer and then added conc. H_2SO_4 drop wise to adjust the pH in the range of 7.5-8.5. The precipitated silica was washed with warm water and dried at 50 ºC for 48 h in oven.

Synthesis of graphene oxide (GO): After the process of nanosilica particles synthesis, the remaining portion of carbon was washed with water and dried in an oven. The carbonized sample powder (2 g) was dissolved in 100 mL of conc. H_2SO_4 and then added 1 g of $NaNO_3$ into the solution. The mixture was maintained at 5-10 ºC for 3 h with constant stirring. After that 6 g of $KMnO_4$ was added slowly in the controlled temperature condition and stirred for 4 h. Then, it was warmed to room temperature stirred continuously in a water bath at 35-40 ºC for 1 h. The prepared solution was diluted by 50 mL of deionized water. Finally, 6 mL of H_2O_2 was added, the yellowish solution started to appear and diluted by 200 mL deionized water. Again washed with 10% HCl followed by centrifuged at 6000 rpm for 20 min. It was ultrasonicated for 30 min and finally drying in a vaccum oven at 60 ºC for 3 h to form graphene oxide.

Preparation of chitosan-nanosilica-graphene oxide (CS-NSi-GO) composite: Nanosilica (3 g) was immersed into 100 mL of water and 3 mL of ammonia solution. The mixer was then dispersed in an ultrasonic bath for 60 min. After the addition of 50 mL graphene oxide aqueous solution dropwisely the mixture was sonicated for 30 min. Then, chitosan (3 g) was completely dissolved by using 3% of 100 mL acetic acid and stirred for 4 h. The prepared solution of nanosilica was drop wise added into the dissolved chitosan. Finally, the NSi-GO solution was added into chitosan solution. The mixture was stirred for 3 h by using magnetic stirrer then the hydrogel was applied at 60 ºC for 3 min to catalyze the hydrolysis and condensation reaction. The resulting gel was dried at 80 ºC chitosan-nanosilica-graphene oxide (CS-NSi-GO) nanocomposite was obtained.

RESULTS AND DISCUSSION

The present work is aimed for the synthesis of pure nanosilica (NSi) and graphene oxide (GO) from the coconut husk ash. Then prepared CS-NSi-GO nanocomposite and characterized by sophisticated analytical techniques like FT-IR, FT-Raman, SEM-EDAX and TEM analysis.

FT- IR studies: The FT- IR spectrum of CS-NSi-GO based nanocomposite is shown in Fig. 1. A strong broad band appeared at 3461 cm^{-1} corresponding to N-H and O-H stretching vibrations as well as the intramolecular hydrogen bond. The peaks at 2877 and 2310 cm^{-1} were attributed to C-H stretching vibration of chitosan. The peak at 1741 cm^{-1} corresponds to the stretching vibration of C=O functional group. The specific peak at 1657 cm-1 is related to the amide (NH-C=O) stretching vibration. The peak at 1562 cm^{-1} is attributed to the N-H bending vibration of NH_2 while the peak at 1405 cm^{-1} corresponds to C-N stretching vibration. The bands at 1384 and 1317 cm^{-1} may be assigned to the symmetric CH_3 deformation and CH bending vibrations. The FTIR spectrum of nanocomposite reveals a new characteristic bands at 1098 and 462 cm^{-1} associated to the stretching vibrations of Si-O-C and Si-O-Si bending mode, respectively. The Si-O-C group emerges from the reaction of COOH from GO and Si-OH from silica. It can be considered that Si-O-C bond can strengthen the interaction between the GO and SiO_2, this evidence proves that the carbonyl groups were converted to Si-O-C bonds. At last, the peak at 618 cm^{-1} corresponds to the symmetric stretching deformation of silica groups.

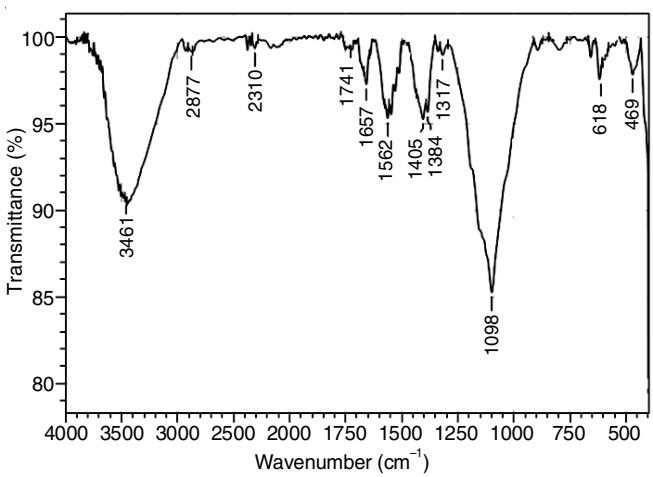

Fig. 1. FT-IR spectrum of CS-NSi-GO nanocomposite

FT- Raman studies: Fig. 2 shows the CS-NSi-GO Raman spectrum. The GO oxidation rate can be displayed through the distinctions in the D and G peak intensities in the Raman spectra. The D-band of the CS-NSi-GO nanocomposite the first peak located at 1305 cm^{-1} corresponds to disorder mode and the G-band located at 1593 cm^{-1} corresponds to the first order E_{2g} mode from sp^2 carbon domains. As can be observed the I_D/I_G degree for the CS-NSi-GO nanocomposite observed in 0.819. Furthermore, the CS-NSi-GO nanocomposite displayed peaks at 1986 cm^{-1}, which can represent C-H vibrations and at 2691 and 2814 cm^{-1}, due to the presence of the chitosan band in the 2D area.

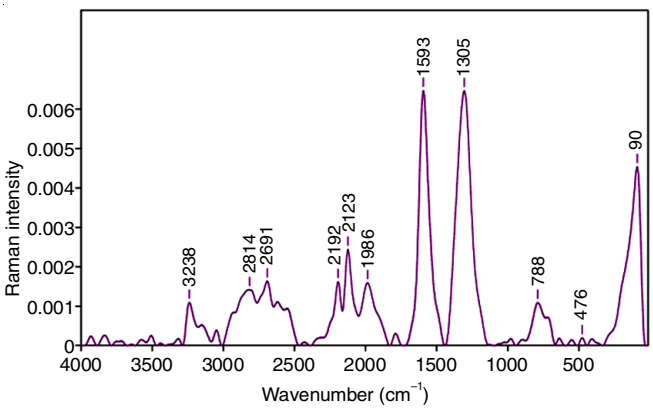

Fig. 2. FT-Raman spectrum of the CS-NSi-GO nanocomposite

SEM studies: Fig. 3 represents the scanning electron microscopic images, which reveals the surface distribution and morphology of the CS-NSi-GO nanocomposite. SEM images shows nanosilica is finely distributed on the surface of GO. These are uniformly distributed on the surface illustrates the successful interaction between the silica, graphene oxide and chitosan.

EDAX studies: Energy dispersive X-ray pattern of the derived CS-NSi-GO nanocomposite is presented in Fig. 4. EDAX analysis clearly confirmed the visible composite surface and the corresponding elements like C, O, N and Ca distributions. The highest peak of oxygen in the EDAX spectrum suggested that oxygen element is predominantly present followed by silica element in high percentage. Small amount of calcium is also observed in the EDAX spectrum since, calcium is from the chitosan which was extracted from a shrimp shell.

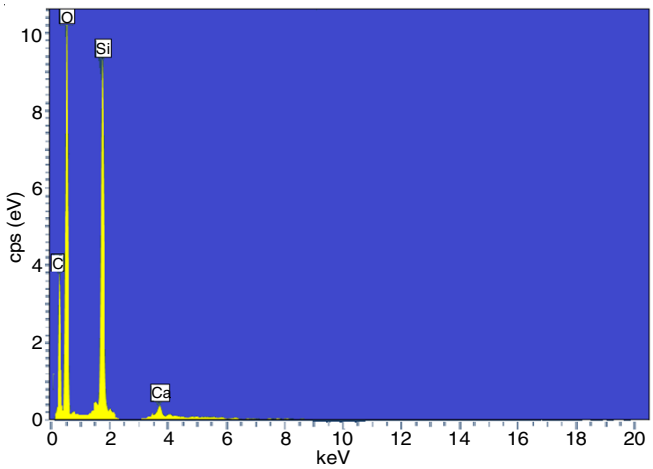

Fig. 4. EDAX images of the CS-NSi-GO nanocomposite

TEM studies: TEM images of the prepared CS-NSi-GO nanocomposite at 50 nm and 100 nm magnifications are shown in Fig. 5. TEM images showed that the silica nanoparticles were spread on the GO layers and clearly visible that the composite material for the network structure. It can be clearly showed that the GO was a sheet-like structure. Chitosan tightly attached to the graphene oxide and nanosilica present in spherical shape.

Antibacterial activity: The antibacterial activity of CS-NSi-GO was screened by dissolving 38 g of Muller Hinton Agar Medium (Hi Media) in 1000 mL of distilled water. The dissolved medium was autoclaved at 15 lbs pressure at 121 ºC

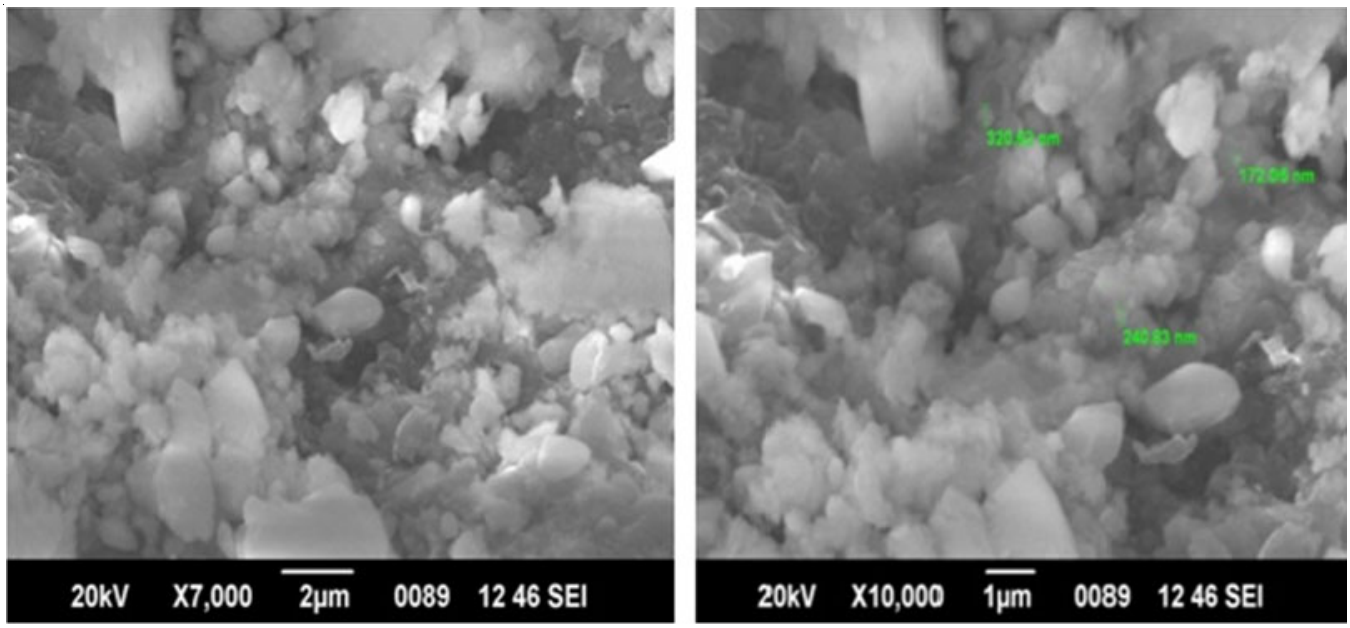

Fig. 3. SEM images of the CS-NSi-GO nanocomposite

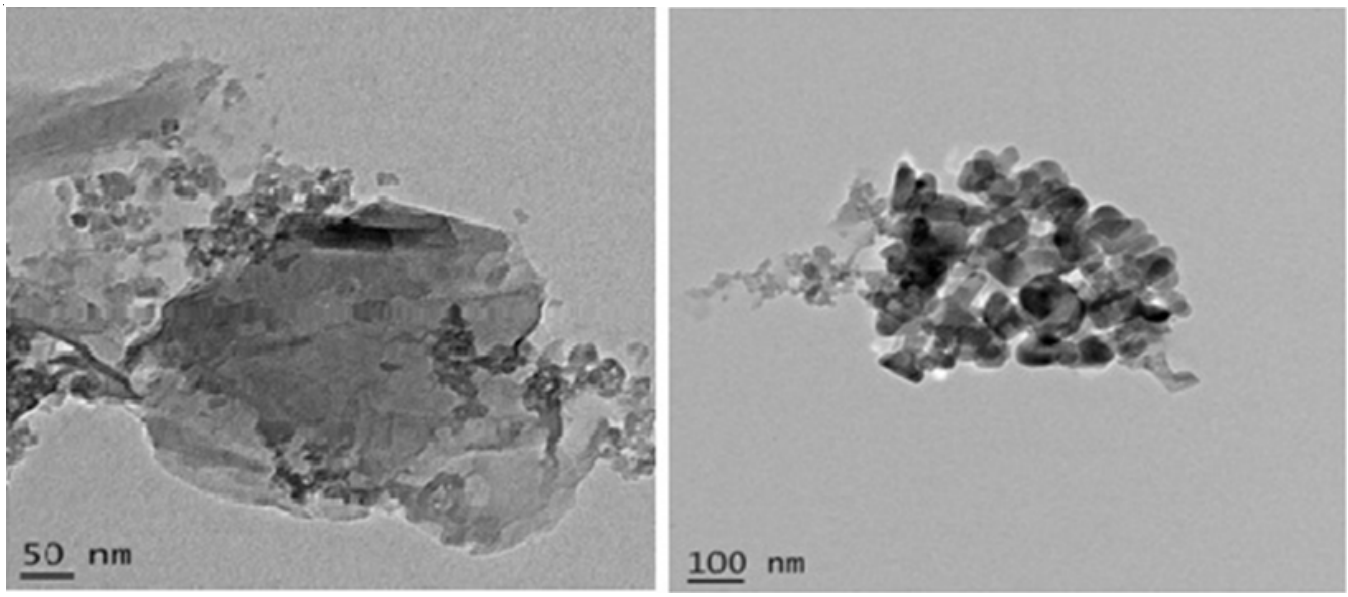

Fig. 5. TEM images of the CS-NSi-GO nanocomposite

for 15 min (pH 7.3). The autoclaved medium was cooled, mixed well and poured petriplates (25 mL/plate), the plate was swabbed with pathogenic bacteria culture *Staphylococcus epidermidis*. Finally, the sample loaded disc was then placed on the surface of Mullar-Hinton medium and the plates were kept for incubation at 37 ºC for 24 h. The size of the zone of inhibition (including disc) was estimated in millimeters. Through serial dilution method, different concentrations (125, 250 and 500 µL) of samples inhibited the growth tested microorganism with a zone of inhibition range from 8 to 12 mm (Fig. 6). At the end of incubation, zone inhibition was observed due to the presence of antibacterial activity.

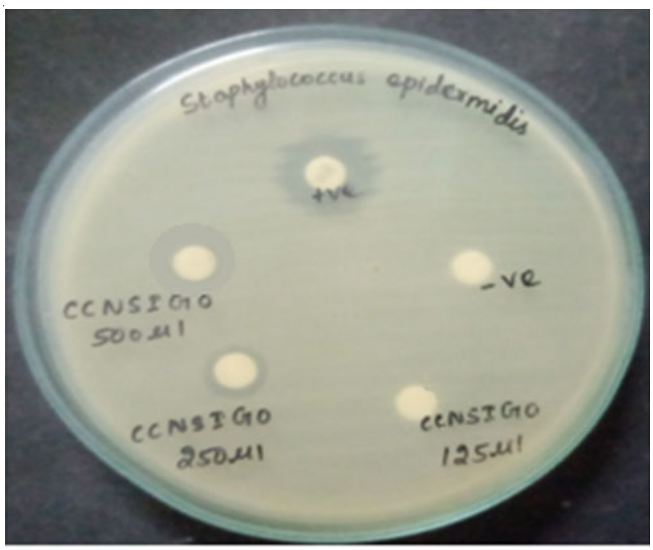

Fig. 6. Antibacterial activity of the different concentrations of CS-NSi-GO against *Staphylococcus epidermidis*

Antifungal activity: Antibiotic susceptibility tests were screened by agar disc diffusion (Kirby-Bauer) method. Fungi strains *Candida albicans* species was swabbed using sterile cotton swabs in SDA agar plate. Up to 40 µL of each concentration of the sample were respectively introduced in the sterile plates utilizing sterile pipettes. The disc was then placed on the surface of SDA medium and the compound was permitted to diffuse for 5 min and the plates were kept for incubation at 22 ºC for 48 h. At the end of incubation, inhibition zones were examined around the disc and estimated with transparent ruler in millimeters. To evaluate antifungal activity with different concentrations (125, 250 and 500 µL) of samples inhibited the growth tested microorganism with a zone of inhibition range 8 mm, 9 mm and 10 mm (Fig.7). At the end of results, zone inhibition was observed due to the presence of antifungal activity.

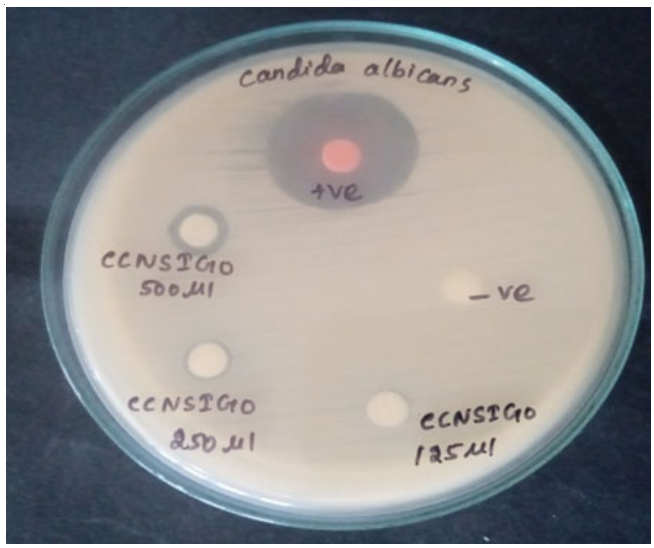

Fig. 7. Antifungal activity of the different concentrations of CS-NSi-GO against *Candida albicans*

Superoxide anion scavenging activity: In the present study, a superoxide radical scavenging assay was supported by riboflavin-light-NBT system. The extract (1 mL) was taken at different concentrations (20, 40, 60, 80 and 100 µg/mL)

and mixed with 0.1 mL of riboflavin (20 µg), 0.2 mL of EDTA solution (12 mM), 0.2 mL of methanol and 0.1 mL of nitro-blue tetrazoliumn (0.5 mM) were mixed and reaction mixture was diluted up to 3 mL with phosphate buffer (50 mM). After 20 min of incubation at room temperature, the absorbance was estimated at 560 nm. Fig. 8 showed that as the nanocomposite concentration increases the scavenging activity also increases. The scavenging ability of the composite was determined by the following equation:

$$\text{Inhibition (\%)} = \frac{OD_{control} - OD_{sample}}{OD_{control}} \times 100$$

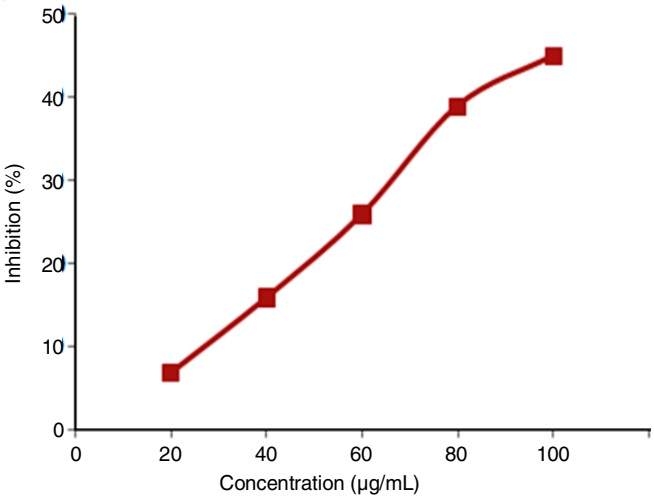

Fig. 8. Superoxide anion scavenging activity of CS-NSi-GO nanocomposite

DPPH Scavenging assay: The antioxidant activity of CS-NSi-GO nanocomposite was determined by evaluating their abilities to free radical scavenging activity of the fractions was measured by 2,2′-diphenyl-1-picrylhydrazyl (DPPH) assay. A DPPH solution (2 mL) were added to both standard and test tubes.Test sample (100 µL) in varying concentration were added to the respective tubes and then stand for 30 min for incubation. After incubation, observe the colour change and measured the absorbance of each tubes at 517 nm. The scavenging ability was concentration dependent and in the range of the The concentration of NSi-GO-CS composite from 20 µg/mL to 100 µg/mL, the scavenging activity increased from 4 to 55% (Fig. 9). The % of inhibition of each concentration was calculated as follows:

$$\text{Inhibition (\%)} = \frac{OD_{control} - OD_{sample}}{OD_{control}} \times 100$$

Nitric oxide scavenging assay: The nitric oxide radical scavenging activity was done using the method of Alderson *et al.* [19]. Nitric oxide is an important chemical intermediate under aerobic condition it combines with oxygen to produce stable compound nitrate and nitrite. Sodium nitroprusside (1 mL of 10 mM) in phosphate buffered saline was mixed with 1 mL of different concentration of extract (20, 40, 60, 80 and 100 µg/mL) and incubated at 25 ºC for 180 min. To a incubation solution, 1 mL of Griess reagent was added and the absorbance

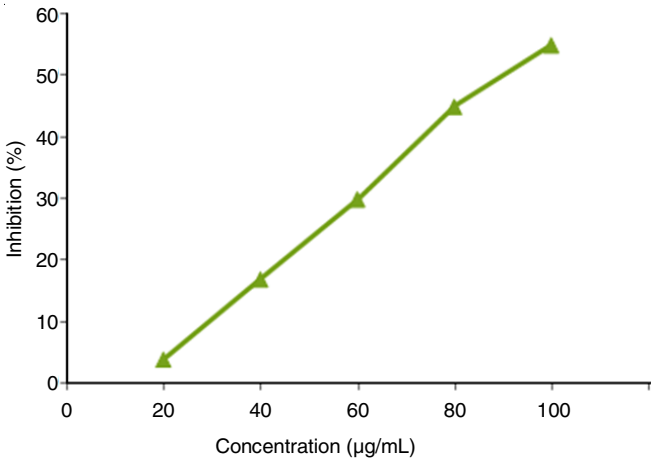

Fig. 9. DPPH scavenging activity of CS-NSi-GO nanocomposite

was measured by UV-spectrometer at 546 nm. The concentration of NSi-GO-CS nanocomposite from 20 µg/mL to 100 µg/mL, the scavenging activity increased from 5 to 50% (Fig. 10). The % of inhibition of each concentration was calculated as follows:

$$\text{Inhibition (\%)} = \frac{OD_{control} - OD_{sample}}{OD_{control}} \times 100$$

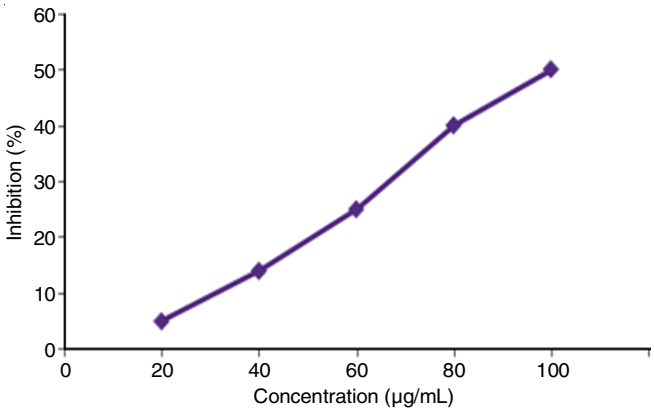

Fig. 10. Nitric oxide scavenging activity of CS-NSi-GO nanocomposite

Cytotoxicity assay by neutral red staining method: The cytotoxicity assay by neutral red staining method is one of the common methods used to distinguish the cell viability or drug cytotoxicity. In brief, after incubation of sample and controls at 37 ± 1 ºC for 24 ± 2 h, the medium was removed and washed gently with 1X washing solution. The washing solution was removed and 150 µL of 1X neutral red staining solution was added to each well and incubated for 2 h. After incubation, the staining solution was removed and the wells were washed with 250 µL of 1X washing solution. A 1X solubilization solution (150 µL) was added to each well and the plate was put in the plate on a shaker for 20 min at room temperature. The absorbance was estimated with microplate reader at 540 nm. The percentage of cell viability was calculated.

Neutral red assay is used to detect the changes in the morphology of the cells, such as rounding or shrinking of cells, granulation and vacuolization in the cytoplasm of the cells

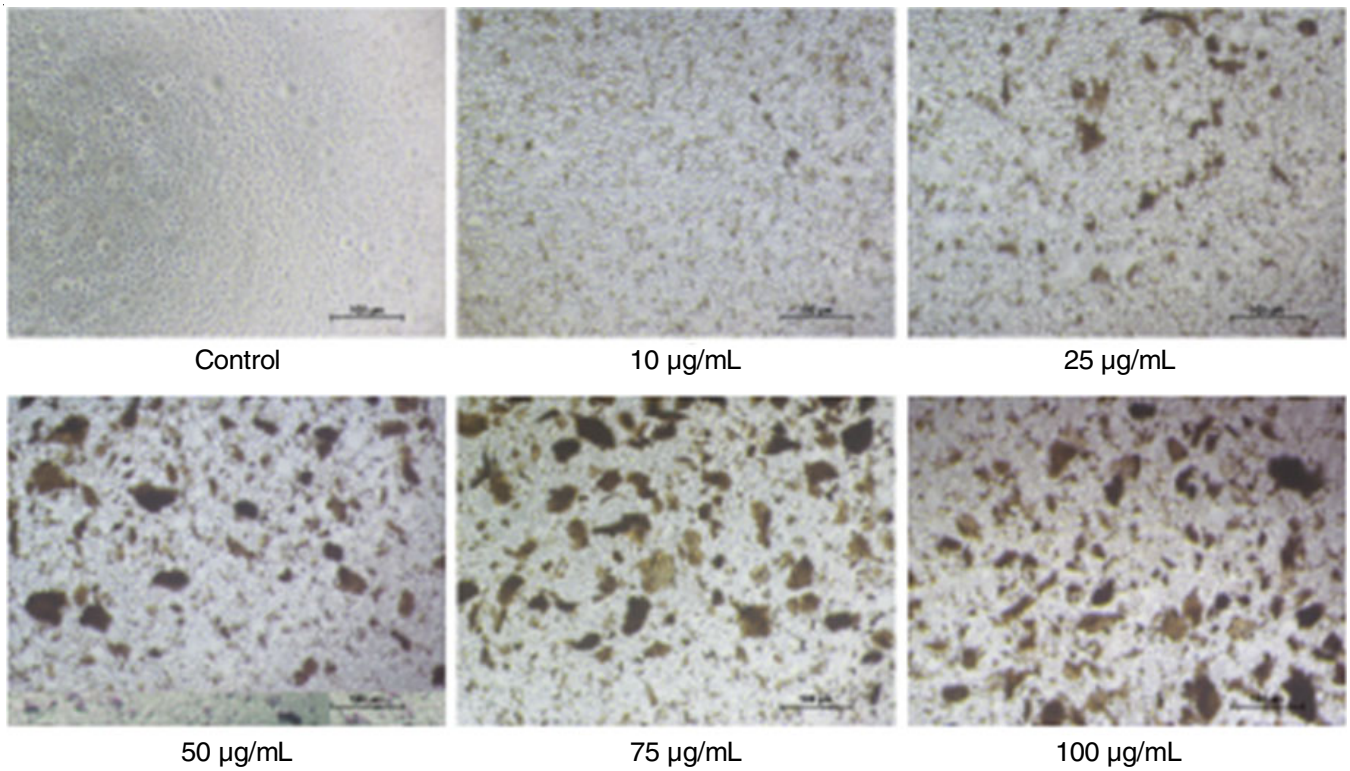

Fig. 12. Morphology of the cell showing the cytotoxicity effect of CS-NSi-GO on L929 (Fibroblast) cells

were considered as indicators of cytotoxicity (Fig. 12). The lower viability % value indicates a higher cytotoxic potential. A sample is considered cytotoxic if the percentage viability value is < 70% and non-cytotoxic, if the percentage viability value is > 70%. For CS-NSi-GO (71.4%) percentage of viable cells observed at highest concentration 100 µg/mL, hence the sample CS-NSi-GO is considered as non-cytotoxic to fibroblast cells (Fig. 11).

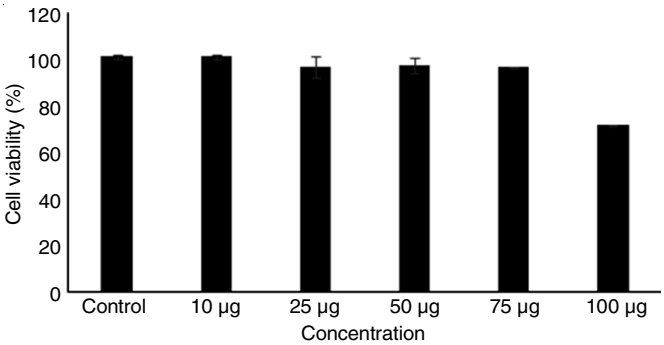

Fig. 11. Cytotoxicity activity of CS-NSi-GO against L929 (Fibroblast) cells

Conclusion

In present study, using nanosilica and graphene oxide from acoconut husk ashes, a CS-NSi-GO nanocomposite was successfully synthesized and characterized. The antibacterial, antifungal, antioxidant and cytotoxicity properties of the nanocomposite were screened and the obtained results indicates excellent antibacterial properties against *Staphylococcus epidermidis* and antifungal properties against *Candida albicans* species. The antioxidant properties were also studied by using superoxide anion radical scavenging activity, DPPH radical scavenging activity and nitric oxide radical scavenging activity confirmed the antioxidant properties of CS-NSi-GO nanocomposite, which is attributed due to the presence of several functional groups. The cytotoxic activity of CS-NSi-GO against L929 (fibroblast) cells a sample is considered non-cytotoxic to fibroblast cells, since it exhibit the percentage of viable cells (71.4%) at the highest concentration 100 µg/mL.

ACKNOWLEDGEMENTS

The authors thank Council of Scientific and Industrial - Research Central Electro Chemical Research Institute (CSIR-CECRI), Karaikudi and Sophisticated Test and Instrumentation Centre Cochin University of Science and Technology, Cochin, India for the material characterization analysis.

CONFLICT OF INTEREST

The authors declare that there is no conflict of interests regarding the publication of this article.

REFERENCES

1. S. Khoee, R. Bafkary and F. Fayyazi, *J. Sol-Gel Sci. Technol.*, **81**, 493 (2017); https://doi.org/10.1007/s10971-016-4213-y
2. N. Morin-Crini, E. Lichtfouse, G. Torri and G. Crini, *Environ. Chem. Lett.*, **17**, 1667 (2019); https://doi.org/10.1007/s10311-019-00904-x
3. A. Suri, V. Khandegar and P.J. Kaur, *Groundw. Sustain. Dev.*, **12**, 100515 (2021); https://doi.org/10.1016/j.gsd.2020.100515
4. J. Diosa, F. Guzman, C. Bernal and M. Mesa, *J. Mater. Res. Technol.*, **9**, 890 (2020); https://doi.org/10.1016/j.jmrt.2019.11.029

5. R.R. Castillo, D. Lozano and M. Vallet-Regí, *Pharmaceutics*, **12**, 432 (2020); https://doi.org/10.3390/pharmaceutics12050432
6. T.M. M. Ways, K.W. Ng, W.M. Lau and V.V. Khutoryanskiy, *Pharmaceutics*, **12**, 751 (2020); https://doi.org/10.3390/pharmaceutics12080751
7. C. Rejeeth, T.C. Nag and S. Kannan, *Cancer Nanotechnol.*, **4**, 127 (2013); https://doi.org/10.1007/s12645-013-0043-6
8. S.A. Qamar, M. Ashiq, M. Jahangeer, A. Riasat and M. Bilal, *Case Stud. Chem. Environ. Eng.*, **2**, 100021 (2020); https://doi.org/10.1016/j.cscee.2020.100021
9. T.M. Budnyak, I.V. Pylypchuk, V.A. Tertykh, E.S. Yanovska and D. Kolodynska, *Nanoscale Res. Lett.*, **10**, 87 (2015); https://doi.org/10.1186/s11671-014-0722-1
10. Q. Xu, T. Ji, S.J. Gao, Z. Yang and N. Wu, *Materials*, **12**, 39 (2018); https://doi.org/10.3390/ma12010039
11. S.K. Tiwari, S. Sahoo, N. Wang and A. Huczko, *J. Sci.-Adv. Mater. Dev.*, **5**, 10 (2020); https://doi.org/10.1016/j.jsamd.2020.01.006
12. K. Narasimharao, G. Venkata Ramana, D. Sreedhar and V. Vasudevarao, *J. Mar. Sci. Eng.*, **5**, 284 (2016); https://doi.org/10.4172/2169-0022.1000284
13. G. Speranza, *J. Carbon Res.*, **5**, 84 (2019); https://doi.org/10.3390/c5040084
14. M. Sabzevari, D.E. Cree and L.D. Wilson, *ACS Omega*, **3**, 13045 (2018); https://doi.org/10.1021/acsomega.8b01871
15. P.P. Zuo, H.F. Feng, Z.Z. Xu, L.F. Zhang, Y.L. Zhang, W. Xia and W.Q. Zhang, *Chem. Cent. J.*, **7**, 39 (2013); https://doi.org/10.1186/1752-153X-7-39
16. D. Yuan, C.M. Ellis and J.J. Davis, *Materials*, **13**, 3795 (2020); https://doi.org/10.3390/ma13173795
17. Y. Du, L. Huang, Y. Wang, K. Yang, Z. Zhang, Y. Wang, M.J. Kipper, L.A. Belfiore and J. Tang, *J. Mater. Sci.*, **55**, 11188 (2020); https://doi.org/10.1007/s10853-020-04774-5
18. C. Brasselet, G. Pierre, P. Dubessay, M. Dols-Lafargue, J. Coulon, J. Maupeu, A. Vallet-Courbin, H. de Baynast, T. Doco, P. Michaud and C. Delattre, *Appl. Sci.*, **9**, 1321 (2019); https://doi.org/10.3390/app9071321
19. W.K. Alderton, C.E. Cooper and R.G. Knowels, *J. Biol. Chem.*, **357**, 593 (2001); https://doi.org/10.1042/0264-6021:3570593